JACS
JOURNAL OF THE AMERICAN CHEMICAL SOCIETY
Communication
pubs.acs.org/JACS

Proton-Assisted Reduction of CO_2 by Cobalt Aminopyridine Macrocycles

Alon Chapovetsky,[‡] Thomas H. Do,[‡] Ralf Haiges,[‡] Michael K. Takase,[†] and Smaranda C. Marinescu*[,‡]

[‡]Department of Chemistry, University of Southern California, Los Angeles, California 90089, United States
[†]Beckman Institute, California Institute of Technology, Pasadena, California 91125, United States

Supporting Information

ABSTRACT: We report here the efficient reduction of CO_2 to CO by cobalt aminopyridine macrocycles. The effect of the pendant amines on catalysis was investigated. Several cobalt complexes based on the azacalix[4](2,6)-pyridine framework with different substitutions on the pendant amine groups have been synthesized (R = H (**1**), Me (**2**), and allyl (**3**)), and their electrocatalytic properties were explored. Under an atmosphere of CO_2 and in the presence of weak Brønsted acids, large catalytic currents are observed for **1**, corresponding to the reduction of CO_2 to CO with excellent Faradaic efficiency (98 ± 2%). In comparison, complexes **2** and **3** generate CO with TONs at least 300 times lower than **1**, suggesting that the presence of the pendant NH moiety of the secondary amine is crucial for catalysis. Moreover, the presence of NH groups leads to a positive shift in the reduction potential of the $Co^{I/0}$ couple, therefore decreasing the overpotential for CO_2 reduction.

Carbon dioxide has received attention as an abundant, economical, and renewable C_1 feedstock, and its catalytic conversion to liquid fuels could positively impact the global CO_2 balance.[1] Much work has gone into developing molecular catalysts for CO_2 reduction[1,2] from inexpensive elements for applications in efficient, scalable energy storage. However, despite promising results in CO_2 reduction, many of these species perform catalysis with low energetic efficiencies and/or low selectivities. Consequently, the development of molecular systems that catalyze the reduction of CO_2 remains a major challenge. In nature, the selective and reversible conversion of CO_2, protons, and reducing equivalents into CO is catalyzed by the enzyme CO-dehydrogenase (CODH), which contains multimetallic active sites.[1b,3] An intermediate in the catalytic cycle of the Ni,Fe-CODH has been characterized by X-ray diffraction (XRD) studies, showing that the CO_2 fragment bridges between Ni and Fe.[4] CO_2 binds to Ni via the C atom and to Fe via one of the carboxylate oxygen atoms. Moreover, the oxygen groups are involved in H-bonding interactions with protonated histidine and lysine residues. Thus, CO_2 binding and catalysis in the enzyme appear to involve bifunctional activation by two metal centers and additional stabilization from proton relays present in the second coordination sphere. In a similar fashion, the pendant amine present in [FeFe]-hydrogenase was shown to assist in proton-transfer steps and facilitate the hydrogen evolution reaction (HER).[1b] These architectural features are instrumental in controlling the protein activity and have inspired the development of molecular systems.

Mononuclear nickel phosphine complexes with pendant proximal bases were reported to catalyze the reduction of protons with turnover frequencies above 100,000 s^{-1}.[5] The mechanism of proton reduction and hydrogen oxidation involves the cooperative interaction of hydrogen with both the metal center and multiple proton relays incorporated in the second coordination sphere, similar to the ones found in hydrogenases.[1d,6] These nickel phosphine complexes were also reported to undergo the electrocatalytic oxidation of formate, and mechanistic studies demonstrate that the pendant amine plays an important role in catalysis.[7] Oxa- and azadithiolate ligands function as proton relays, indicated by the enhanced rates of proton reduction of these species.[8] Recent studies have shown that modification of iron tetraphenylporphyrin through the introduction of eight phenolic groups in all ortho and ortho′ positions of the phenyl groups enhances CO_2 electroreduction to CO.[9] The basis of the enhanced activity was hypothesized to be the high local concentration of protons associated with the phenolic hydroxyl substituents. High reactivities and selectivities were also observed for the reduction of CO_2 by manganese bipyridine complexes with pendant phenols[10] and for the electrocatalytic oxygen reduction reaction by porphyrins or corroles with pendant carboxylic acids.[11] Manganese complexes that include a coordinated carboxamide as a proton shuttle were reported to catalyze the O_2 reduction.[12] Other reactions have been recently facilitated through the use of noncovalent interactions between a substrate and the secondary sphere of transition-metal complexes, such as iridium or iron species, which were reported to catalyze the hydrogenation of CO_2,[13] the dehydrogenation of formic acid or alcohols,[14] or both.[15] Metal complexes with pendant borane groups were shown to facilitate the reductive coupling of CO[16] and the dehydrogenation of ammonia borane.[17]

We became interested in macrocyclic aminopyridine ligands, such as azacalix[4](2,6)pyridines, due to the promising precedents in the CO_2 reduction chemistry of several pyridine[18] and macrocyclic complexes.[1a−c] Macrocyclic compounds based on azacalix[4](2,6)pyridines have been developed recently in the context of supramolecular host−guest interaction and molecular recognition.[19] However, their catalytic properties have not been explored. We report here the efficient reduction of CO_2 by cobalt aminopyridine macrocycles.

Received: February 22, 2016
Published: April 19, 2016

DOI: 10.1021/jacs.6b01980
J. Am. Chem. Soc. 2016, 138, 5765−5768

The desired ligands were prepared according to the reported literature procedures.[19] Several ligands with different substitutions on the pendant amines were employed (R = H ($\mathbf{L^1}$), Me ($\mathbf{L^2}$), and allyl ($\mathbf{L^3}$)). Addition of cobalt(II) precursors to the macrocyclic aminopyridines $\mathbf{L^{1-3}}$ led to the formation of the corresponding metal complexes (**1**−**3**) in near quantitative yields (eq 1). Single crystal XRD studies of **1**−**3** reveal that the four

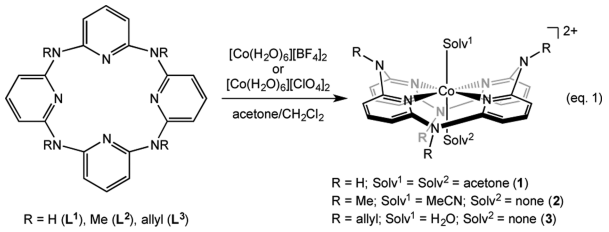

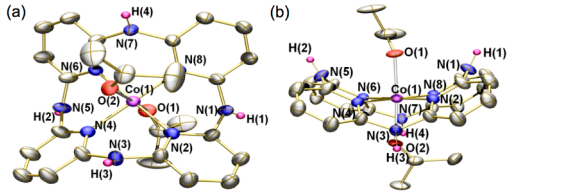

Figure 1. (a) Top and (b) side views of the solid-state structure of **1**. Hydrogen atoms, noncoordinating anions, and solvent molecules are omitted for clarity.

pyridine nitrogen atoms coordinate in a square planar fashion, with Co−N bond lengths of about 1.9(1) Å (Figure 1). The ClO_4^- or BF_4^- counteranions are outside the coordination sphere. The azacalix[4](2,6)pyridine ligands adopt a saddle conformation with approximate D_{2d} symmetry, if the axial ligands are not taken into account. Complexes **1**−**3** feature a solvent molecule(s) coordinated in the axial position(s). The nonbonding Co−N(pendant amine) distances range between 2.9−3.1 Å.

Cyclic voltammograms (CVs) of **1** using a glassy carbon electrode (GCE) in a dimethylformamide (DMF) solution of 0.1 M $[n\mathrm{Bu_4N}][PF_6]$ under a nitrogen atmosphere feature a reversible peak at −1.59 V and an irreversible peak at −2.36 V (Figures 2a, S1−3). All the potentials are listed versus $Fc^{+/0}$. They can be converted to SCE by the addition of 0.45 V.[20] To determine whether these peaks correspond to cobalt or to a ligand based reduction, the zinc analogue, $[Zn(L^1)][BF_4]_2$, was synthesized, and its electrochemistry was explored. No peaks were observed in the CVs of the zinc analogue between potentials of 0 and −2.8 V (Figure S4), suggesting that the

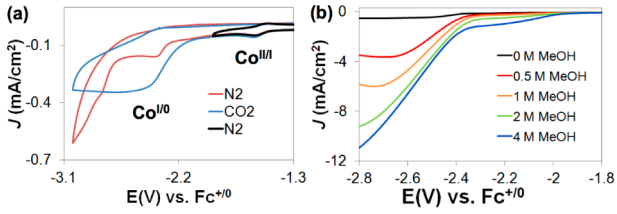

Figure 2. Electrochemical studies of **1**. (a) CVs of **1** (0.5 mM) in 0.1 M $[n\mathrm{Bu_4N}][PF_6]$ in DMF under N_2 (black and red) or CO_2 (blue). (b) Linear scan voltammograms of **1** (0.5 mM) in 0.1 M $[n\mathrm{Bu_4N}][PF_6]$ in DMF under CO_2 and varying concentrations of methanol. Scan rates: 100 mV/s.

reduction events observed at −1.59 and −2.36 V can be assigned to $Co^{II/I}$ and $Co^{I/0}$ couples, respectively.

CVs of **1** under CO_2 (1 atm) exhibit enhanced currents at potentials near that of the $Co^{I/0}$ reduction (Figure 2a). Addition of weak Brønsted acids such as methanol (Figure 2b) or 2,2,2-trifluoroethanol (TFE) (Figures S7−9) to **1** resulted in large increases in current. A current density of 10 mA/cm^2 was achieved at −2.75 V in the presence of **1** (0.5 mM), MeOH (4 M), and CO_2 (1 atm). This current increase corresponds to the reduction of CO_2 to CO, as verified by controlled potential electrolysis (CPE), further discussed below. The normalized peak catalytic current (i_{cat}/i_p) is related to the TOF of the catalytic reaction, which is 370(40) s^{-1}, as derived from CV data using the reported formula (see SI).[21] CVs in the absence of catalyst or CO_2 exhibit no current increase indicating that the activity is not due to the blank GCE or to proton reduction (Figure S5). At high methanol concentrations, the current densities reach a limiting value independent of alcohol concentration, which is typical of saturation kinetics expected for catalytic reactions (Figures S6, S9). Catalytic current densities increase linearly with catalyst loading (Figures S10−11), consistent with a reaction that is first order in catalyst. Analogous catalytic currents similar to the ones in DMF are observed in other solvents, such as a 1:4 mixture of DMF and acetonitrile and dimethyl sulfoxide (DMSO) (Figures S12−14).

CPE of **1** (0.5 mM) was performed at a potential of −2.8 V in a DMF solution containing $[n\mathrm{Bu_4N}][PF_6]$ (0.1 M) and TFE (1.2 M) under CO_2 atmosphere (Figure S16). 30.9 coulombs of charge were consumed after 2 h. Analysis of the gas mixture in the headspace of the working compartment of the electrolysis cell by gas chromatography confirmed production of CO with a Faradaic efficiency (FE) of 98 ± 2% and a total TON ($mol_{CO}/mol_{cat.}$) of 6.2(1) (Table 1). Only trace amounts of H_2 were

Table 1. Electrochemical Studies of 1−3

Cat.	$E_{1/2}(Co^{II/I})$	$E(Co^{I/0})$	i_{cat}/i_p	TOF_{CV}[a] (s^{-1})	F.E.(%)	Total TON	TOF_{CPE}[b] (s^{-1})	TON[b]
1	−1.59	−2.36	43	360(40)	98(2)	6.2(1)	170(20)	$1.22(1)\times10^6$
2	−1.41	−2.58	20	78(8)	23(2)	0.3(1)	0.5(1)	$3.60(3)\times10^3$
3	–	–	–	–	<1(1)	–	<0.0016(2)	<12(1)

[a]Derived using the equations reported in ref 21. [b]Derived using the equations reported in refs 2b and 9a (see SI).

detected. The liquid phase was also analyzed, but no CO-containing products were detected. Additionally, trace amounts of CO were detected in the headspace of the auxiliary electrode compartment of the CPE cell. Negligible current densities and CO amounts were observed using the cobalt(II) starting material or in the absence of **1** (Table S3, Figure S17). Complex **1** affords a continuous increase in the charge build-up over the course of 2 h, suggesting that **1** is moderately stable in longer-duration CPE. Approximately 72(5)% of catalyst **1** remains in the DMSO-d_6 solution after the 2 h CPE, as indicated by ^{1}H NMR spectroscopy and electrochemical studies (Figures S32−33). The GCE used in the CV or CPE experiments of **1** was rinsed with DMF (3 ×), and its electrochemistry was measured in fresh DMF solutions (Figures S18−19). Very low current densities were observed, suggesting that complex **1** does not deposit on the GCE during catalysis to generate a modified electrode active for the reduction of CO_2. Additionally, CPE of **1** in the presence of mercury showed no change in catalytic activity, suggesting that **1** does not generate cobalt particles active for catalysis. The TOF, derived from CPE data using the reported formula,[2b,9a] is 170(20) s^{-1}

DOI: 10.1021/jacs.6b01980
J. Am. Chem. Soc. 2016, 138, 5765−5768

(see SI for details). Complex **1** generates CO with a 1.22(1) million TON over the course of 2 h. The reduction potential for the CO_2/CO couple is −0.73 V,[9a,c,22] and thus taking into account the pK_a of the alcohols, the overpotential for the reduction of CO_2 with **1** ranges between 0.35 and 0.68 V with MeOH and TFE, respectively (see SI).

To understand the effect of the pendant amine on the catalysis, the electrochemistry of complexes **2** and **3** was explored and compared to that of **1**. CVs of **2** under N_2 feature a reversible peak at −1.41 V, assigned to the $Co^{II/I}$ redox couple, and an irreversible peak at −2.58 V, assigned to the $Co^{I/0}$ reduction (Table 1 and Figures S20−21). The $Co^{I/0}$ reduction is shifted to more negative potentials relative to that of **1**, as expected for substitutions with electron-donating groups such as methyls. CVs of **2** under CO_2 (1 atm) exhibit enhanced currents at potentials near that of the $Co^{I/0}$ reduction. Addition of alcohols to **2** leads to small current enhancements relative to the ones observed for complex **1** (Figures S22−23). CPE studies of **2** display currents lower than those of **1** (Figure S16). Analysis of the gas mixture indicates CO production with a FE of only 23 ± 2% (Table 1), a TOF of 0.5(1) s^{-1}, and a TON of 3600(30) over 2 h. Negligible amounts of H_2 were detected. After rinsing the electrode with DMF (3×), negligible current densities were obtained (Figure S25), suggesting that complex **2** does not deposit during catalysis.

The electrochemistry of complex **3** displays only irreversible reduction events, which prohibits the proper assignment (Figures S26). The ill-defined electrochemical behavior of **3** could be due to the propensity of the pendant olefin to coordinate to the reduced Co species and/or undergo isomerization of the double bond or due to the formation of allyl radicals. CVs of **3** under CO_2 exhibit similar currents with the ones under N_2, suggesting weak binding of CO_2 by the reduced species of **3**. Additionally, CPE studies of **3** display small currents and trace amounts of CO (negligible TOF and TON), suggesting that complex **3** is a poor catalyst for CO_2 reduction. Moreover, after rinsing the electrode with DMF (3×), similar current densities were obtained (Figure S29), suggesting that **3** decomposes to a heterogeneous mixture during electrocatalysis.

A proposed mechanism for the reduction of CO_2 to CO by **1** is illustrated in Figure 3. Complex **1** is reduced by one electron to generate $[Co(L^1)]^+$ (**4**), which can be reduced further to $[Co(L^1)]$. Enhanced currents are observed at potentials near that for the $Co^{I/0}$ couple upon addition of CO_2, suggesting that $[Co(L^1)]$ can bind the substrate to form $[Co(L^1)(CO_2)]$ (**5**). CO_2 was shown previously to coordinate to a cobalt(I) tetraazamacrocyclic complex and form a CO_2 adduct that has been spectroscopically characterized.[1c,23] IR studies performed by Fujita et al. indicate the presence of intramolecular H-bonding between bound CO_2 and the macrocycle in solution at low temperature.[24] In a similar fashion, we propose that the bound CO_2 fragment in **5** is stabilized by intramolecular H-bonds of the pendant secondary amines. For tertiary amines, as in the case of complexes **2** and **3**, this stabilization cannot occur, which is in agreement with our experimental results. Species **5** can then undergo a two-electron transfer to generate $[Co(L^1)(CO_2^{2-})]$. This type of intermediate was observed by Fujita et al. for a cobalt tetraazamacrocyclic complex using XANES.[25] In the presence of protons this intermediate is converted into a metal-CO_2H species (**6**). Proton-promoted C−OH bond cleavage gives a carbonyl complex, which subsequently dissociates CO to regenerate the starting material **1**. The moderate durability of **1** in longer-duration CPE could be due to catalyst deactivation by CO, which was observed for $[Ni(cyclam)]^{2+}$ by Kubiak et al. using infrared spectroelectrochemical studies.[26] For complexes **2** and **3** different protonation sites (*exo*- and *endo*-protonation) are possible, as observed for the nickel phosphine complexes, that could also have a detrimental effect on catalysis.[27]

In an attempt to isolate any proposed intermediates, excess KC_8 was added to **1** in DMF, which led to a rapid color change from orange to blue. The ^{1}H NMR spectrum of the reaction mixture in pyridine-d_5 indicates complete consumption of the starting material **1**. Three broad paramagnetic peaks at δ 33.4, 11.2, and 4.8 ppm are observed in the 2:1:1 ratio. X-ray quality crystals were grown by vapor diffusion from a pyridine/diethyl ether mixture. Single crystal XRD studies confirm the formation of the Co(I) species **4** (Figure 4). Complex **4** displays an octahedral environment, with four pyridine groups of the macrocycle ligand, L^1, in the equatorial plane (Co−N_{eq} = 1.97(1) Å) and two pyridine molecules in the axial positions (Co−N_{ax} = 2.23(2) Å). The BF_4^- counteranion is outside the coordination sphere. The nonbonding Co−N(pendant amine) distances are ∼3.1(1) Å. The nickel phosphine complexes with pendant proximal bases, which were reported to catalyze the efficient reduction of protons, display nonbonding Ni−N distances of 3.2−3.4 Å,[6a] which are comparable to the Co−N distances observed in complexes **1**−**4** reported here. CVs of **4** in the presence of CO_2, or CO_2 and protons (TFE), exhibit similar currents with the ones observed for **1**, suggesting that **4** is kinetically competent (Figures S34−35). Attempts to isolate proposed intermediate **5** by stoichiometric reactions have been unsuccessful to date. Nevertheless, the effect of the pendant H-bonding donors on catalytic activity is clear when the performance of **1** is compared to **2** and **3**, which are missing the NH moieties. Complex **1** generates CO with a TON that is about 300× higher than **2**, even though complex **2** has a more

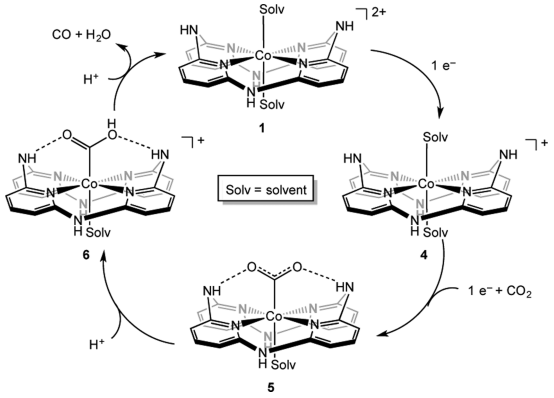

Figure 3. A proposed mechanism for the reduction of CO_2 using **1**.

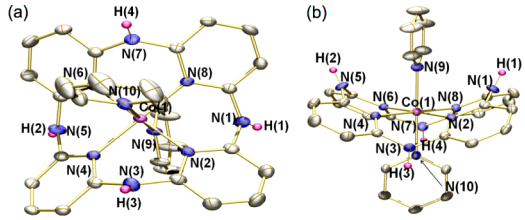

Figure 4. (a) Top and (b) side views of the solid-state structure of **4**. Hydrogen atoms, noncoordinating anions, and solvent molecules are omitted for clarity.

DOI: 10.1021/jacs.6b01980
J. Am. Chem. Soc. 2016, 138, 5765−5768

negative $Co^{I/0}$ reduction potential than **1** (by 0.22 V). Complex **3** generates negligible amounts of CO. In a similar fashion, CO_2 activation in CODH is assisted by H-bonding interactions.[1b,3]

In summary, several cobalt macrocyclic compounds based on azacalix[4](2,6)pyridines have been synthesized, and their electrocatalytic properties were explored. Complex **1** catalyzes the reduction of CO_2 to CO with excellent Faradaic efficiency. Our studies indicate that the cobalt system with pendant NH groups is at least 2 orders of magnitude more efficient than the systems with pendant *N*-alkyl groups (Me or allyl). Moreover, the presence of NH groups leads to a positive shift in the reduction potential of the $Co^{I/0}$ couple, therefore decreasing the overpotential for CO_2 reduction. Mechanistic studies of the CO_2 reduction by cobalt aminopyridine systems are under investigation.

■ ASSOCIATED CONTENT

Supporting Information

The Supporting Information is available free of charge on the ACS Publications website at DOI: 10.1021/jacs.6b01980.

Experimental procedures, spectroscopic characterization, and electrochemical data (PDF)
Crystallographic data (PDF)

■ AUTHOR INFORMATION

Corresponding Author

*smarines@usc.edu

Notes

The authors declare no competing financial interest.

■ ACKNOWLEDGMENTS

This work was supported by the University of Southern California and the National Science Foundation (NSF) through the NSF CAREER award (CHE−1555387). We are grateful to the USC Wrigley Institute for a Norma and Jerol Sonosky summer fellowship to A.C. We thank Catherine Bridges for the synthesis of a batch of ligand precursor. We are grateful to NSF (grant CRIF 1048807) and USC for their sponsorship of NMR spectrometers and X-ray diffractometer. We are grateful to Anton Burg Foundation for their sponsorship of the elemental analysis instrument.

■ REFERENCES

(1) (a) Benson, E. E.; Kubiak, C. P.; Sathrum, A. J.; Smieja, J. M. *Chem. Soc. Rev.* **2009**, *38*, 89. (b) Appel, A. M.; Bercaw, J. E.; Bocarsly, A. B.; Dobbek, H.; Dubois, D. L.; Dupuis, M.; Ferry, J. G.; Fujita, E.; Hille, R.; Kenis, P. J.; Kerfeld, C. A.; Morris, R. H.; Peden, C. H.; Portis, A. R.; Ragsdale, S. W.; Rauchfuss, T. B.; Reek, J. N.; Seefeldt, L. C.; Thauer, R. K.; Waldrop, G. L. *Chem. Rev.* **2013**, *113*, 6621. (c) Morris, A. J.; Meyer, G. J.; Fujita, E. *Acc. Chem. Res.* **2009**, *42*, 1983. (d) Rakowski DuBois, M.; DuBois, D. L. *Acc. Chem. Res.* **2009**, *42*, 1974.

(2) (a) Collin, J. P.; Sauvage, J. P. *Coord. Chem. Rev.* **1989**, *93*, 245. (b) Costentin, C.; Robert, M.; Savéant, J.-M. *Chem. Soc. Rev.* **2013**, *42*, 2423. (c) Savéant, J.-M. *Chem. Rev.* **2008**, *108*, 2348.

(3) Ragsdale, S. W.; Kumar, M. *Chem. Rev.* **1996**, *96*, 2515.

(4) Jeoung, J.-H.; Dobbek, H. *Science* **2007**, *318*, 1461.

(5) Helm, M. L.; Stewart, M. P.; Bullock, R. M.; DuBois, M. R.; DuBois, D. L. *Science* **2011**, *333*, 863.

(6) (a) Rakowski DuBois, M.; DuBois, D. L. *Chem. Soc. Rev.* **2009**, *38*, 62. (b) Wilson, A. D.; Shoemaker, R. K.; Miedaner, A.; Muckerman, J. T.; DuBois, D. L.; DuBois, M. R. *Proc. Natl. Acad. Sci. U. S. A.* **2007**, *104*, 6951. (c) Dubois, D. L. *Inorg. Chem.* **2014**, *53*, 3935.

(7) (a) Galan, B. R.; Schoffel, J.; Linehan, J. C.; Seu, C.; Appel, A. M.; Roberts, J. A.; Helm, M. L.; Kilgore, U. J.; Yang, J. Y.; DuBois, D. L.; Kubiak, C. P. *J. Am. Chem. Soc.* **2011**, *133*, 12767. (b) Seu, C. S.; Appel, A. M.; Doud, M. D.; DuBois, D. L.; Kubiak, C. P. *Energy Environ. Sci.* **2012**, *5*, 6480.

(8) Barton, B. E.; Olsen, M. T.; Rauchfuss, T. B. *J. Am. Chem. Soc.* **2008**, *130*, 16834.

(9) (a) Costentin, C.; Drouet, S.; Robert, M.; Savéant, J.-M. *Science* **2012**, *338*, 90. (b) Costentin, C.; Passard, G.; Robert, M.; Savéant, J.-M. *J. Am. Chem. Soc.* **2014**, *136*, 11821. (c) Costentin, C.; Passard, G.; Robert, M.; Savéant, J.-M. *Proc. Natl. Acad. Sci. U. S. A.* **2014**, *111*, 14990.

(10) Agarwal, J.; Shaw, T. W.; SchaeferIII, H. F.; Bocarsly, A. B. *Inorg. Chem.* **2015**, *54*, 5285.

(11) (a) Rosenthal, J.; Nocera, D. G. *Acc. Chem. Res.* **2007**, *40*, 543. (b) Zhao, M.; Wang, H.-B.; Ji, L.-N.; Mao, Z.-W. *Chem. Soc. Rev.* **2013**, *42*, 8360. (c) Dogutan, D. K.; Stoian, S. S.; McGuire, R.; Schwalbe, M.; Teets, T. S.; Nocera, D. G. *J. Am. Chem. Soc.* **2011**, *133*, 131. (d) Carver, C. T.; Matson, B. D.; Mayer, J. M. *J. Am. Chem. Soc.* **2012**, *134*, 5444. (e) Rigsby, M. L.; Wasylenko, D. J.; Pegis, M. L.; Mayer, J. M. *J. Am. Chem. Soc.* **2015**, *137*, 4296.

(12) (a) Shook, R. L.; Peterson, S. M.; Greaves, J.; Moore, C.; Rheingold, A. L.; Borovik, A. S. *J. Am. Chem. Soc.* **2011**, *133*, 5810. (b) Borovik, A. S. *Acc. Chem. Res.* **2005**, *38*, 54.

(13) (a) Schmeier, T. J.; Dobereiner, G. E.; Crabtree, R. H.; Hazari, N. *J. Am. Chem. Soc.* **2011**, *133*, 9274. (b) Ahn, S. T.; Bielinski, E. A.; Lane, E. M.; Chen, Y.; Bernskoetter, W. H.; Hazari, N.; Palmore, G. T. R. *Chem. Commun.* **2015**, *51*, 5947. (c) Zhang, Y.; MacIntosh, A. D.; Wong, J. L.; Bielinski, E. A.; Williard, P. G.; Mercado, B. Q.; Hazari, N.; Bernskoetter, W. H. *Chem. Sci.* **2015**, *6*, 4291.

(14) (a) Bielinski, E. A.; Lagaditis, P. O.; Zhang, Y.; Mercado, B. Q.; Würtele, C.; Bernskoetter, W. H.; Hazari, N.; Schneider, S. *J. Am. Chem. Soc.* **2014**, *136*, 10234. (b) Bielinski, E. A.; Förster, M.; Zhang, Y.; Bernskoetter, W. H.; Hazari, N.; Holthausen, M. C. *ACS Catal.* **2015**, *5*, 2404. (c) Chakraborty, S.; Lagaditis, P. O.; Förster, M.; Bielinski, E. A.; Hazari, N.; Holthausen, M. C.; Jones, W. D.; Schneider, S. *ACS Catal.* **2014**, *4*, 3994. (d) Sharninghausen, L. S.; Mercado, B. Q.; Crabtree, R. H.; Hazari, N. *Chem. Commun.* **2015**, *51*, 16201.

(15) Hull, J. H.; Himeda, Y.; Wang, W.-H.; Hashiguchi, B.; Periana, R.; Szalda, D. J.; Muckerman, J. T.; Fujita, E. *Nat. Chem.* **2012**, *4*, 383.

(16) (a) Miller, A. J. M.; Labinger, J. A.; Bercaw, J. E. *Organometallics* **2010**, *29*, 4499. (b) Miller, A. J. M.; Labinger, J. A.; Bercaw, J. E. *J. Am. Chem. Soc.* **2008**, *130*, 11874.

(17) Conley, B. L.; Guess, D.; Williams, T. J. *J. Am. Chem. Soc.* **2011**, *133*, 14212.

(18) (a) Hawecker, J.; Lehn, J.-M.; Ziessel, R. *Helv. Chim. Acta* **1986**, *69*, 1990. (b) Smieja, J. M.; Kubiak, C. P. *Inorg. Chem.* **2010**, *49*, 9283. (c) Elgrishi, N.; Chambers, M. B.; Artero, V.; Fontecave, M. *Phys. Chem. Chem. Phys.* **2014**, *16*, 13635.

(19) (a) Miyazaki, Y.; Kanbara, T.; Yamamoto, T. *Tetrahedron Lett.* **2002**, *43*, 7945. (b) Uchida, N.; Zhi, R.; Kuwabara, J.; Kanbara, T. *Tetrahedron Lett.* **2014**, *55*, 3070. (c) Zhang, E.-X.; Wang, D.-X.; Huang, Z.-T.; Wang, M.-X. *J. Org. Chem.* **2009**, *74*, 8595. (d) Gong, H.-Y.; Zhang, X.-H.; Wang, D.-X.; Ma, H.-W.; Zheng, Q.-Y.; Wang, M.-X. *Chem. - Eur. J.* **2006**, *12*, 9262.

(20) Connelly, N. G.; Geiger, W. E. *Chem. Rev.* **1996**, *96*, 877.

(21) (a) Sampson, M. D.; Nguyen, A. D.; Grice, K. A.; Moore, C. E.; Rheingold, A. L.; Kubiak, C. P. *J. Am. Chem. Soc.* **2014**, *136*, 5460. (b) Sampson, M. D.; Kubiak, C. P. *J. Am. Chem. Soc.* **2016**, *138*, 1386.

(22) Pegis, M. L.; Roberts, J. A. S.; Wasylenko, D. J.; Mader, E. A.; Appel, A. M.; Mayer, J. M. *Inorg. Chem.* **2015**, *54*, 11883.

(23) Fujita, E.; Szalda, D. J.; Creutz, C.; Norman, S. *J. Am. Chem. Soc.* **1988**, *110*, 4870.

(24) Fujita, E.; Creutz, C.; Sutin, N.; Brunschwig, B. S. *Inorg. Chem.* **1993**, *32*, 2657.

(25) Fujita, E.; Furenlid, L. R.; Renner, M. W. *J. Am. Chem. Soc.* **1997**, *119*, 4549.

(26) Froehlich, J. D.; Kubiak, C. P. *J. Am. Chem. Soc.* **2015**, *137*, 3565.

(27) Brown, H. J. S.; Wiese, S.; Roberts, J. A. S.; Bullock, R. M.; Helm, M. L. *ACS Catal.* **2015**, *5*, 2116.

DOI: 10.1021/jacs.6b01980
J. Am. Chem. Soc. 2016, 138, 5765−5768